Fatigue Fract. Engng Mater. Struct. Vol. 13, No. 3, pp. 287–296, 1990
Printed in Great Britain.

8756-758X/90 $3.00 + 0.00

EFFECT OF SPECIMEN GEOMETRY ON FATIGUE CRACK GROWTH IN PLANE STRAIN—I. CONSTANT AMPLITUDE RESPONSE

H. R. SHERCLIFF and N. A. FLECK
Cambridge University Engineering Department, Trumpington Street, Cambridge CB2 1PZ, England

(*Received in final form* 23 *October* 1989)

Abstract—The influence of specimen geometry on crack growth and crack closure response was determined for BS4360 50B steel and 6082-T6 aluminium alloy. Specimens were sufficiently thick for plane strain conditions to prevail along most of the crack front. After an initial crack growth transient from the sharpened notch, and steady state conditions are attained, the growth rate and closure responses are independent of specimen geometry. At growth rates above the near-threshold regime the cyclic crack openings exceed the fracture surface roughness for the steel, but are much less than the surface roughness for the aluminium alloy. This suggests that roughness-induced crack closure plays a dominant role for the aluminium alloy but not for the steel. Finally, the effect of mean stress upon closure response is presented for the steel.

NOMENCLATURE

a = crack length
E = Young's modulus
$K, \Delta K$ = stress intensity factor (range)
N = number of cycles
$P, \Delta P$ = load (range)
r_{pc} = cyclic plastic zone size
R = R ratio (P_{min}/P_{max})
T = T-stress
U = closure ratio
W = specimen width (Bend), half-width (CCP)
σ = applied stress
σ_{xx} = normal stress parallel to crack
σ_y = yield stress
$\Delta\delta$ = cyclic crack opening displacement

Subscripts
eff = effective
min = minimum
max = maximum
N = notch
ol = overload
op = opening

INTRODUCTION

Fatigue crack propagation in metals and polymers has generally been quantified in terms of the stress intensity factor, K. Recent finite element studies [1] have shown that in addition to K the geometry can affect fatigue crack propagation. The magnitude of higher order terms in the near-tip asymptotic elastic stress field depends on geometry, in particular the non-singular stress parallel

to the crack, known as the "T-stress". It is the dominant stress experienced on the crack flanks since the singular terms vanish there. In an elastic analysis using the Finite Element Method (FEM) the T-stress may be calculated by extrapolating the stress σ_{xx} on the crack flanks to the crack tip. FEM analysis suggests that in plane strain the T-stress can influence the crack closure response, and therefore the crack growth rate.

Fatigue crack closure

It is found experimentally that a fatigue crack can remain shut for part of the fatigue cycle, even for tensile–tensile loading. The portion of the fatigue cycle for which the crack is open, ΔK_{eff}, provides the driving force for crack growth. The closure ratio U is defined as

$$U = \frac{K_{\max} - K_{\text{op}}}{K_{\max} - K_{\min}} = \frac{\Delta K_{\text{eff}}}{\Delta K} \tag{1}$$

where $K_{\max}$, $K_{\min}$, K_{op} are the maximum, minimum and crack opening stress intensity factors, respectively.

Closure has been attributed to a number of sources: oxide debris, fatigue surface roughness, and the residual plastic wake of the crack tip plastic zone. There is no general agreement over the occurrence of closure in plane strain. It is argued that plastic deformation occurring at constant volume cannot provide the extra material needed to cause crack closure, under plane strain conditions. However, residual plastic strains in the loading direction can exist if they are balanced by residual elastic strains in the crack wake or by material displacements remote from the crack [2]. It is therefore argued that plasticity-induced crack closure may have a significant influence on fatigue crack propagation in plane strain.

Finite element studies

Previous work using the finite element method is described in Refs [1, 2]. Both the centre-cracked panel (CCP) and Bend specimen were considered, see Fig. 1. FEM predictions were made of the closure response at constant ΔK amplitude and load ratio $R = 0$ under conditions of both plane stress and plane strain. Figure 2 shows the predicted initial closure response for plane stress and for plane strain. Consistently higher closure loads are shown for plane stress than for plane strain

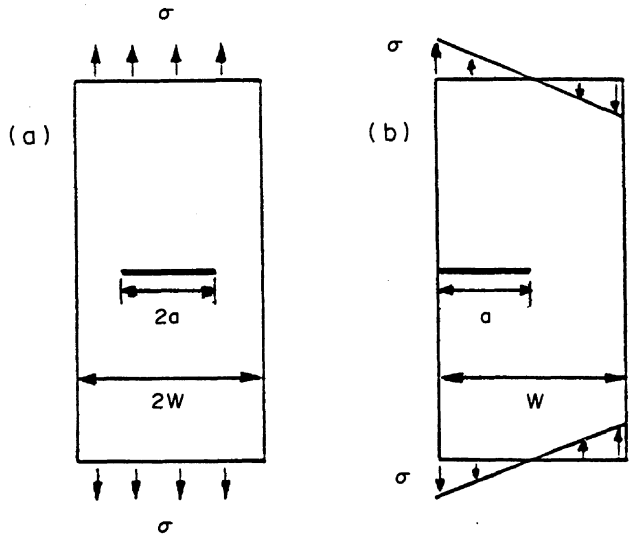

Fig. 1. Specimen geometries analysed by FEM. (a) Centre cracked panel. (b) Bend specimen.

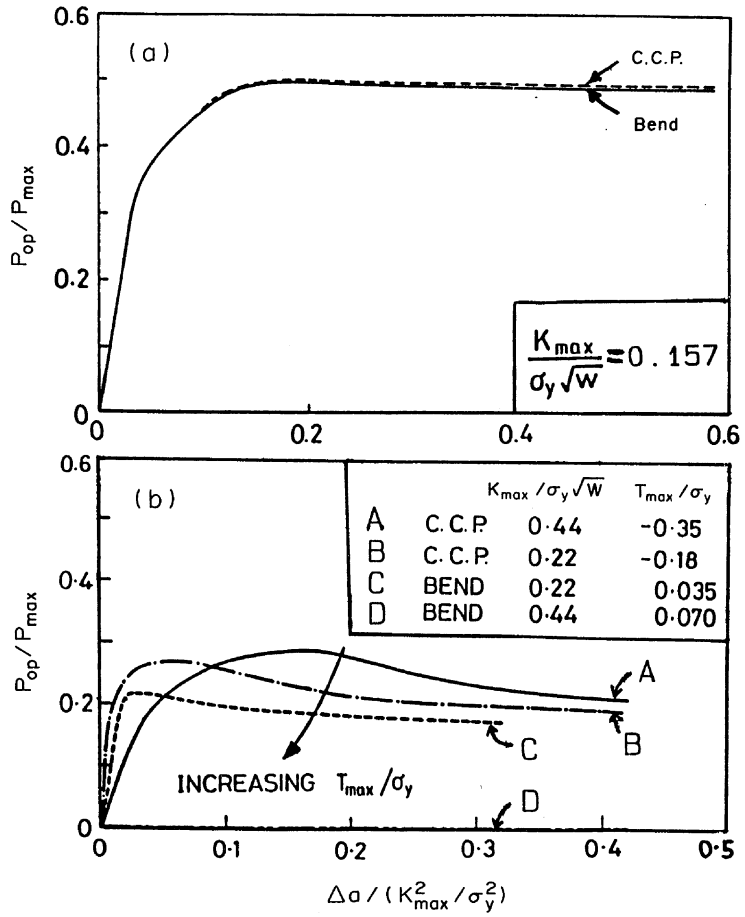

Fig. 2. Crack opening response predicted by FEM at constant ΔK ($R = 0$) for CCP and Bend geometries: (a) plane stress; (b) plane strain.

conditions. The initial transient varied with specimen geometry for plane strain but not for plane stress conditions. The geometry dependence in plane strain was correlated with the normalised T-stress, T_{max}/σ_y, at $K = K_{max}$ of the fatigue cycle by Fleck and Newman [1], see Fig. 2(b). Fleck and Newman showed that for both plane stress and plane strain conditions, the final cyclic plastic zone size is similar for the two geometries, implying that geometry has no effect on constant amplitude growth rate. In the finite element studies [1, 2] the number of elements suffering forward yield at the crack tip was typically 200, and the number of elements suffering reversed yield was 100, with 10 yielded elements directly ahead of the crack tip. Use of diagonal elements obviates the problem of plane strain locking associated with incompressible plastic flow. Thus we have some confidence in the accuracy of the finite element computations.

Figure 3 shows the amplitude of normalised crack tip displacement against R ratio, taken from the work of Fleck and Newman by extrapolating the cyclic crack opening to the crack tip. Only the response at the end of the initial transient is presented. The influence of geometry is again small, and so no difference in growth rate is anticipated. Note that the value of normalised $\Delta\delta$ is close to 0.5 which is consistent with simple analytical solutions (e.g. as quoted in Ref. [3]). The FEM solution predicts a small decrease in cyclic crack opening with decreasing R ratio due to closure, with a slightly stronger influence in the CCP geometry than in the Bend. It is anticipated that the relative magnitude of the cyclic crack opening and the fatigue surface roughness strongly influences the closure behaviour. This will be discussed further in the Constant Load Tests section.

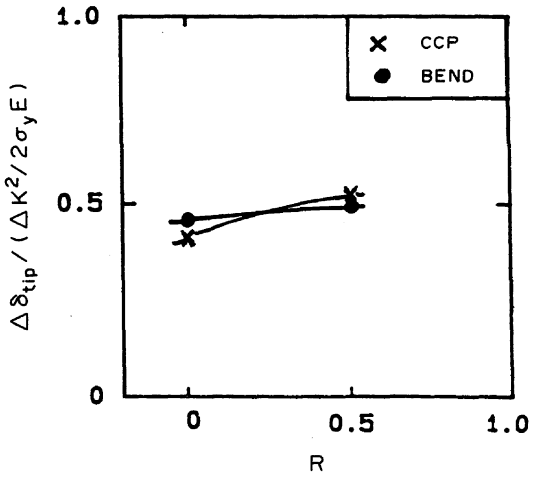

Fig. 3. Normalised cyclic crack tip opening displacement predicted by FEM.

From the finite element calculations, two questions emerge:

1. What is the effect of specimen geometry on the steady state crack growth and closure responses, in plane strain?
2. What is the role of fracture surface roughness on closure response?

The present work attempts to answer in part these two fundamental questions.

TEST METHODS

Compact tension (CT) and centre-cracked panel specimens were made from 6082-T6 aluminium alloy and BS4360 50B structural steel.

The nominal compositions and mechanical properties are given in Table 1. Note that alloy 6082 is similar to U.S. alloy 6061. The aluminium alloy was used in the as-received condition and had a thickness of 9.9 mm, while the steel was machined down to thicknesses of 16 and 12 mm from 25 mm plate. Further specimen details are as follows: for the CCP (Al alloy), width $2W = 100$ mm, crack length $2a = 10$–40 mm while for the CCP (steel), $2W = 150$ mm, $2a = 35$–60 mm and for the Bend specimens (both materials), width $W = 50$ mm, crack length $a = 15$–35 mm. In both

Table 1. Composition and mechanical properties of alloys

6082 aluminium alloy		BS4360 50B steel	
Element	Wt (%)	Element	Wt (%)
Si	0.7–1.3	C	0.14
Mg	0.6–1.2	Mn	1.27
Mn	0.4–1.0	Si	0.41
Fe	<0.5	P	0.017
Cu	<0.1	S	0.004
Zn	<0.2	Al	0.073
Al	balance	Fe	balance

Property	6082-T6 aluminium	BS4360 50B steel
0.2% proof/yield stress (MPa)	280–300	352
Tensile strength (MPa)	320–340	519
Elongation (%)	12	36

materials, cracks were grown normal to the rolling direction. All steel specimens were in the normalised condition and were stress relieved at 650°C for 1.5 h prior to testing.

Servo-hydraulic fatigue machines of various load capacities were used. All tests were in load control, with loads controlled manually. Test frequencies were between 5 and 10 Hz.

Crack length at the surface was measured to a resolution of 10 μm with a travelling microscope. Crack length on the back surface was measured by microscope in a few tests, otherwise a visual check was made that the crack was growing sensibly straight during the test. This was also assessed by inspection of the fatigue surface after specimen failure. Crack growth rates were calculated by 7-point quadratic fit to the data in accordance with ASTM E-647. Crack closure was monitored using near-tip clip gauges; that is both a crack mouth clip gauge and a near-tip Elber gauge. In addition for CT specimens a back face strain gauge was used. The offset procedure and low-pass filters were used to improve the accuracy of the closure measurements [4].

Roughness measurements were made on the fatigue surfaces using a Ferranti Surfcom machine.

CONSTANT LOAD TESTS

Tests were performed on both materials at constant load range ΔP. Results for the 6082-T6 aluminium alloy are shown in Fig. 4, and results for the BS4360 50B steel are given in Fig. 5.

It is apparent from Fig. 4 that specimen geometry has no significant influence on the da/dN vs ΔK or da/dN vs ΔK_{eff} responses, for crack growth rates in the range 10^{-6} mm/cycle to 10^{-3} mm/cycle. However, constant load range tests are prone to scatter in crack growth rates by a factor of approximately 2.

The da/dN vs ΔK response for the 6082-T6 aluminium alloy shows a kink at $\Delta K = 8$ MPa$\sqrt{\text{m}}$. It is suggested that this kink occurs when the cyclic plastic zone, r_{pc}, is of similar size to the dislocation subgrain size, following Ewalds and Wanhill [3]. Since $r_{pc} = (1/2\pi)(\Delta K/2\sigma_y)^2$ this corresponds to $r_{pc} = 28\ \mu$m, which is of the correct order.

The crack opening load ratio P_{op}/P_{max} rises steeply with decreasing ΔK for the aluminium alloy but not for the steel, compare Figs 4(b) and 5(b). A comparison of the crack tip cyclic displacements $\Delta\delta$ with the fracture surface roughness, Fig. 6, shows that roughness-induced crack closure is much more significant for the aluminium alloy than for the steel. It is deduced from Ref. [1] that the cyclic crack openings do not change much in the near crack tip region; the cyclic opening at a distance of the cyclic plastic zone size behind the crack tip is less than twice the crack tip value.

We conclude that roughness-induced crack closure dominates for the aluminium alloy but plasticity-induced crack closure dominates for the steel. This is consistent with the observation that P_{op}/P_{max} falls steeply with increasing ΔK for the aluminium alloy, but remains constant at 0.2 for ΔK in the range 10–30 MPa$\sqrt{\text{m}}$ for the steel.

CONSTANT ΔK TESTS

Constant ΔK tests were conducted in order to measure da/dN and P_{op}/P_{max} more accurately than in constant load tests. In the constant ΔK tests loads were shed manually after crack growth increments of 0.1–0.2 mm. Typical test results are given in Fig. 7 (further results at other ΔK and R values are reported in Ref. [5]).

We find that for the two geometries considered, under LEFM conditions, the steady state crack growth rate and closure response are independent of specimen geometry. The crack growth or closure measurement techniques were unsuitable for detecting the initial transient in response, when the crack had advanced less than 0.5 mm from the sharpened saw-cut notch.

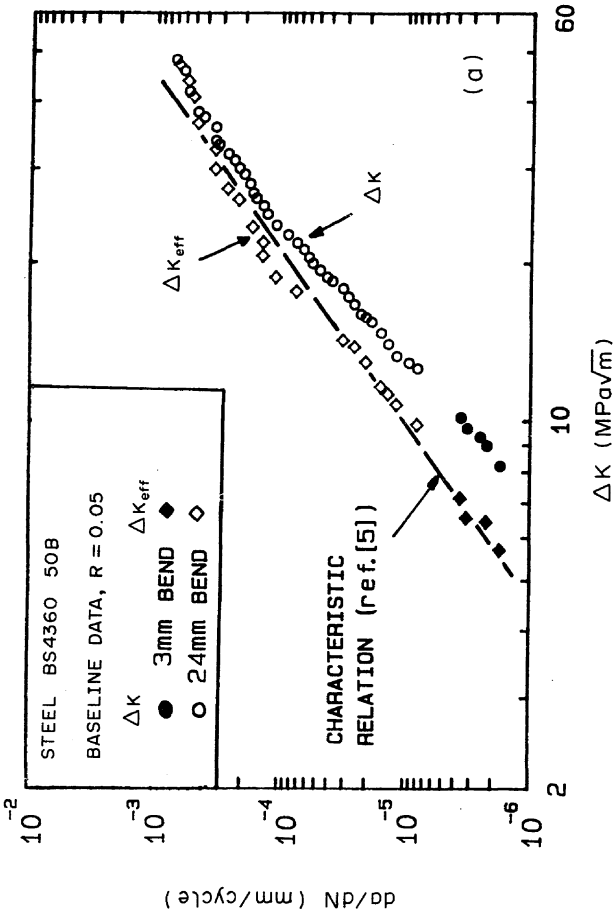

Fig. 5. Baseline data at constant load amplitude, ΔP at $R = 0.05$, for steel BS 4360 50B. Data for Bend specimens only are shown. (a) Crack growth rate da/dN against ΔK and ΔK_{eff}; (b) crack opening response, P_{op}/P_{max} against ΔK.

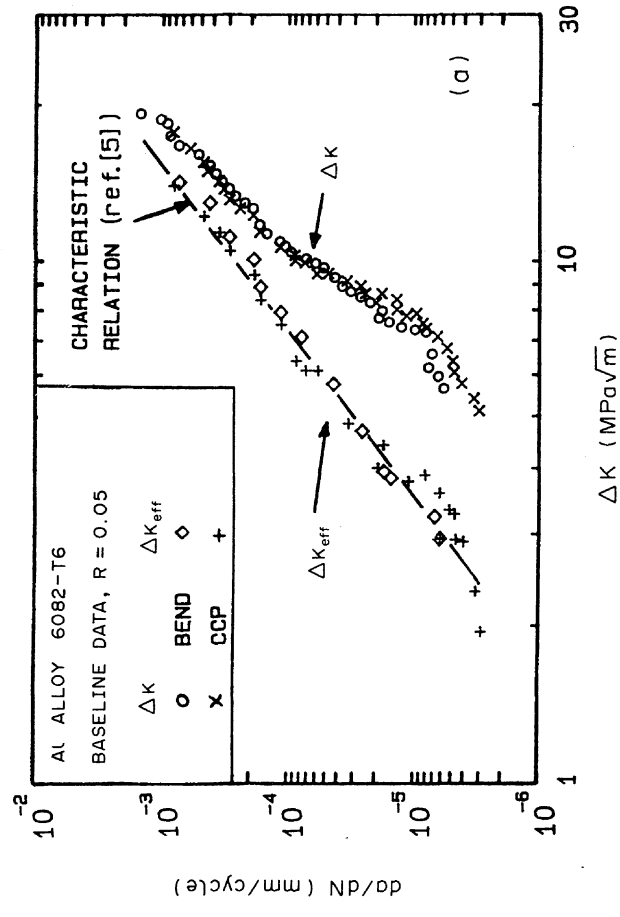

Fig. 4. Baseline data at constant load amplitude ΔP at $R = 0.05$, for aluminium alloy 6082-T6. Data for both CCP and Bend specimens are shown. (a) Crack growth date da/dN against ΔK and ΔK_{eff}; (b) crack opening response, P_{op}/P_{max} against ΔK.

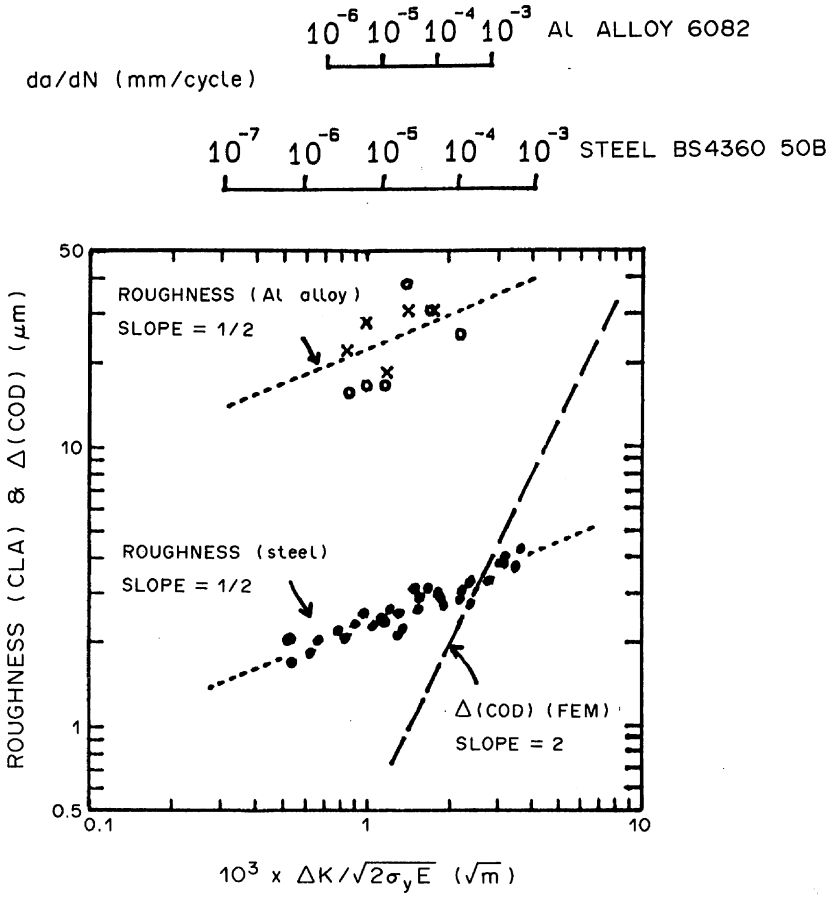

Fig. 6. Data for roughness in terms of the centre-line average (CLA) against $\Delta K/\sqrt{2\sigma_y E}$ for aluminium alloy 6082-T6 and steel BS 4360 50B from tests at constant load amplitude (the corresponding crack growth rates for the two materials are indicated above the diagram). The predicted cyclic crack opening response from FEM is also shown.

It appears that specimen geometry may exert an influence (via differences in T-stress) on the initial transient but not upon steady state response. The finite element calculations of Fleck and Newman [1] showed that residual plasticity in the crack wake led to large residual tensile stresses behind the crack tip parallel to the crack plane *in both geometries*. Thus we may expect specimen geometry to exert less effect on the steady state closure and crack growth response than upon the initial transient response.

We note in Fig. 7 that the crack growth rate and closure loads in constant ΔK tests are in good agreement with the results from constant load tests.

EFFECT OF MEAN STRESS

For completeness the effect of mean load on the crack growth and closure response of BS4360 50B steel is shown in Fig. 8. The tests were performed on 24 mm thick CT specimens. Tests at crack growth rates above 10^{-5} mm/cycle were performed at constant load range while tests at lower growth rates were done using a load shed procedure with $(1/K)(dK/da) = -0.08\ \text{mm}^{-1}$.

We deduce from Fig. 8 that an increase in mean stress causes a small increase in da/dN and in the fraction of the load cycle for which the crack is open, $U = \Delta K_{\text{eff}}/\Delta K$. The da/dN vs ΔK_{eff} relation, Fig. 8(b), is preserved implying that crack closure can account for the influence of mean stress in a satisfactory manner. Three regimes are shown in the closure response, Fig. 8(c). Regime I refers to the near threshold closure response, where the U value drops steeply with decreasing

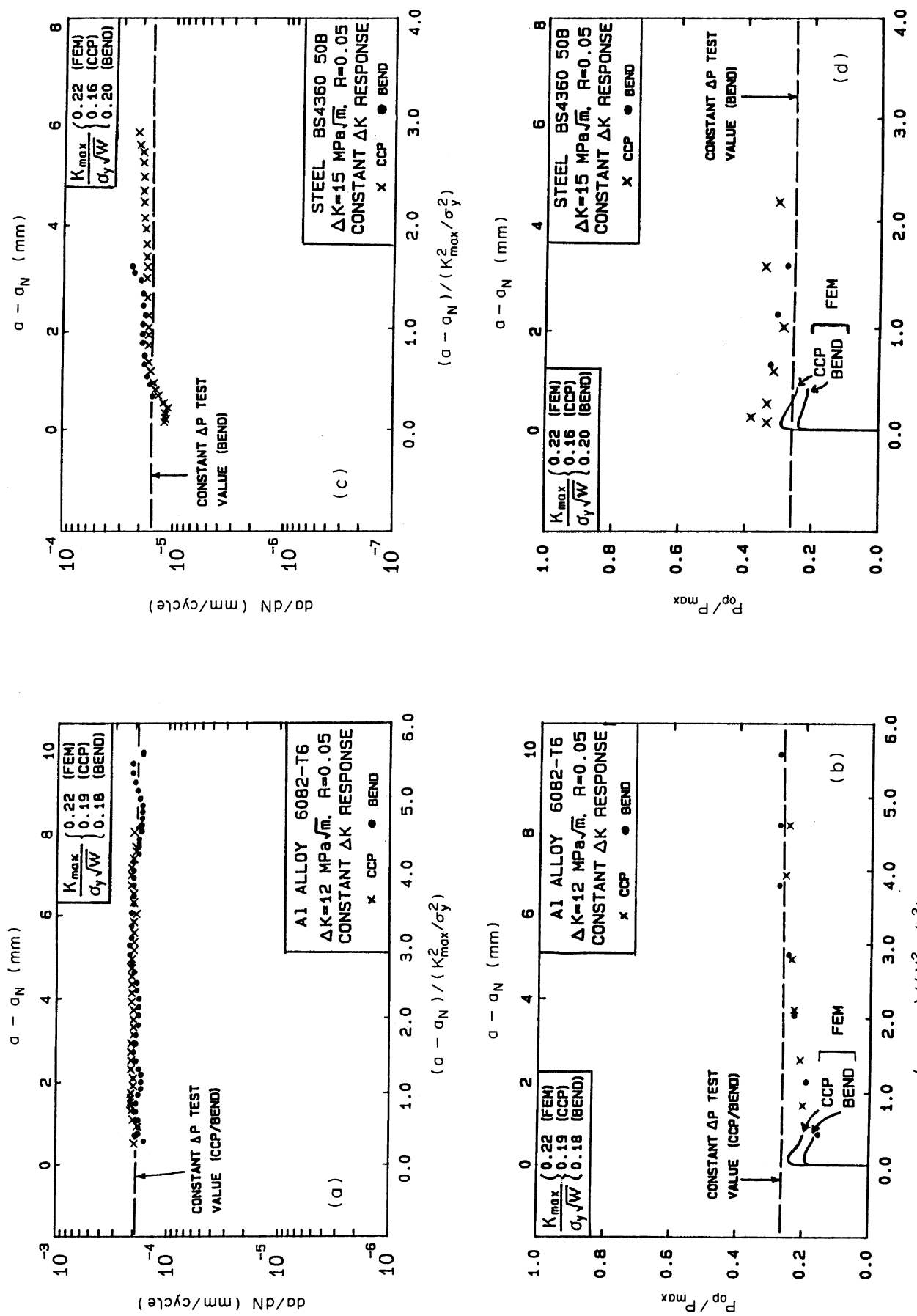

Fig. 7. Comparison of constant amplitude ΔK response for CCP and Bend geometries showing crack growth rate and opening response against normalised crack growth increment (from notch length a_N). The values expected from constant load baseline data, and the FEM predicted crack opening are also included.

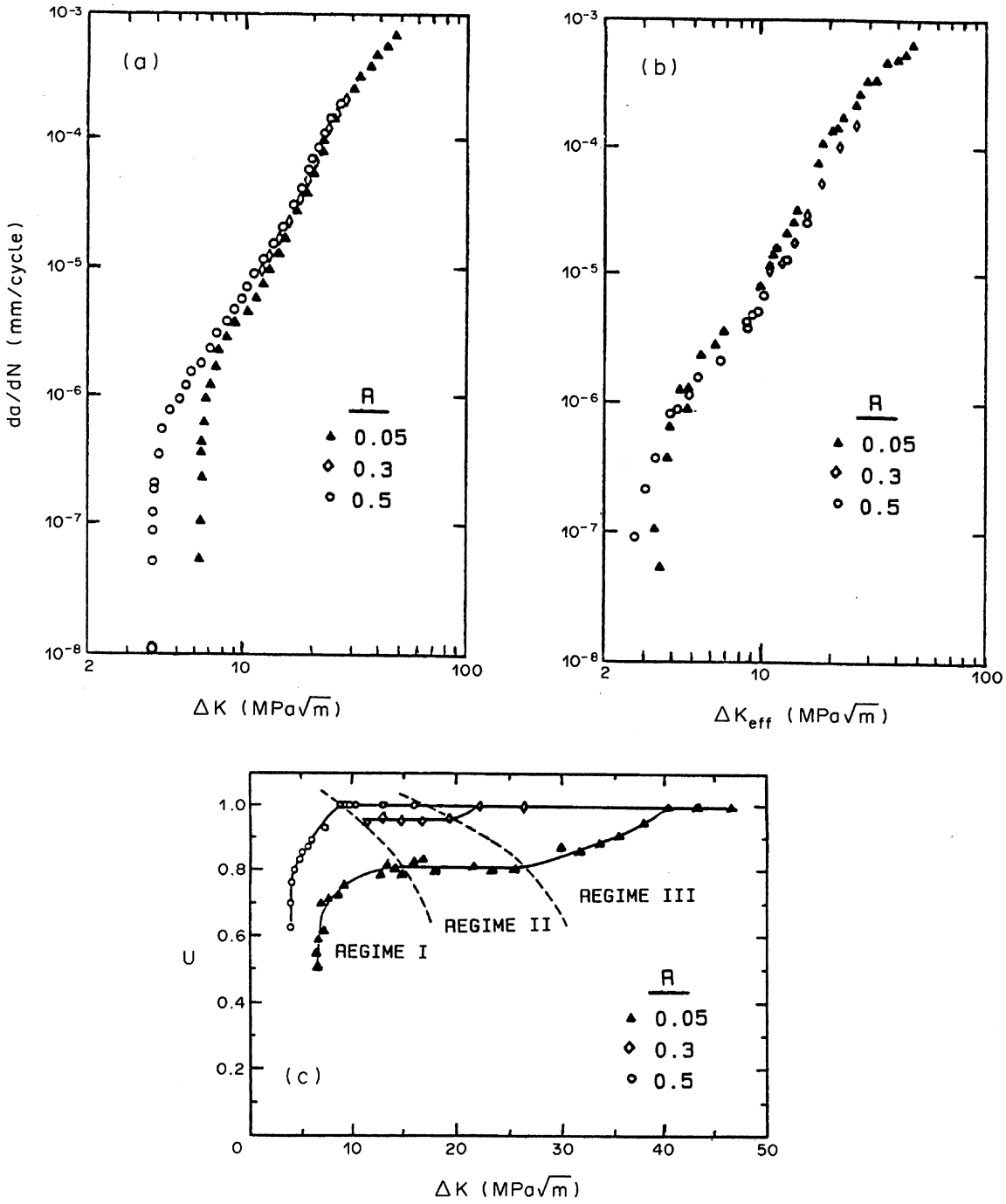

Fig. 8. Effect of mean stress on crack growth rate and closure responses of 24 mm thick BS 4360 50B steel (Bend specimens).

ΔK. Such behaviour is due to the dominance of oxide-induced and roughness induced crack closure. In regime II, plasticity-induced closure dominates and the closure value U is independent of ΔK, as predicted by dimensional analysis; see Ref. [1].

It seems likely that loss of closure ($U \rightarrow 1$) in regime III is due to the finite size of the test-piece. When the crack tip plastic zone is large relative to the size of the specimen, the surrounding elastic field is insufficient to close the crack. Supporting evidence comes from the study of Fujitani *et al.* [6] on high strength maraging steels. They found that the closure value U increased to unity as their CT specimens approached net section yield. This view is also supported by the finite element calculations of Lalor and Sehitoglu [7].

CONCLUSIONS

We conclude that specimen geometry has no significant influence on the crack growth or closure responses of long cracks in 6082-T6 aluminium alloy or BS4360 50B steel, under plane strain conditions. This substantiates the use of ΔK as a correlating parameter in plane strain.

Surface roughness measurements indicate that roughness-induced crack closure is much more significant in the aluminium alloy than in the steel.

Acknowledgements —The authors wish to thank NASA Langley Research Centre, Virginia, U.S.A., and Dr J. C. Newman Jr for financial support via Grant No. NAGW-1014.

REFERENCES

1. N. A. Fleck and J. C. Newman, Jr (1988) Analysis of crack closure under plane strain conditions. *Mechanics of Fatigue Crack Closure* (Edited by J. C. Newman Jr. and W. Elber), *ASTM STP 982*, pp. 319–341. ASTM, Philadelphia, Pa.
2. N. A. Fleck (1986) Finite element analysis of plasticity-induced crack closure under plane strain conditions. *Engng Fract. Mech.* **25,** 441–449.
3. H. L. Ewalds and R. J. H. Wanhill (1985) *Fracture Mechanics*, pp. 281–282. Edward Arnold, London.
4. N. A. Fleck (1982) The use of compliance and electrical resistance techniques to characterise fatigue crack closure. Cambridge Univ. Engng Dept, Rep. CUED/C-Mat/TR89.
5. H. R. Shercliff and N. A. Fleck (1989) The effect of geometry on fatigue crack growth in plane strain. Cambridge Univ. Engng Dept, Rep. CUED/C-Mat/TR150.
6. K. Fujitani, T. Sakai, A. Nakagawa and T. Tanaka (1982) Effect of specimen thickness on fatigue crack propagation in high strength steels. *Bull. J.S.M.E.* **25,** 1195–1201.
7. P. L. Lalor and H. Sehitoglu (1988) Fatigue crack closure outside a small-scale yielding regime. *Mechanics of Fatigue Crack Closure* (Edited by J. C. Newman Jr and W. Elber), *ASTM STP 982*, pp. 342–360. ASTM, Philadelphia, Pa.